Amide-modified prenylcysteine based Icmt inhibitors: Structure–activity relationships, kinetic analysis and cellular characterization

Jaimeen D. Majmudar [a,b,†], Heather B. Hodges-Loaiza [b,c,†], Kalub Hahne [b,c], James L. Donelson [a,c], Jiao Song [a,c], Liza Shrestha [a,c], Marietta L. Harrison [a,c], Christine A. Hrycyna [b,c,*], Richard A. Gibbs [a,c,*]

[a] Department of Medicinal Chemistry and Molecular Pharmacology, Purdue University, West Lafayette, IN 47907, United States
[b] Department of Chemistry, Purdue University, West Lafayette, IN 47907, United States
[c] The Purdue University Center for Cancer Research, Purdue University, West Lafayette, IN 47907, United States

ABSTRACT

Human protein isoprenylcysteine carboxyl methyltransferase (hIcmt) is the enzyme responsible for the α-carboxyl methylation of the C-terminal isoprenylated cysteine of CaaX proteins, including Ras proteins. This specific posttranslational methylation event has been shown to be important for cellular transformation by oncogenic Ras isoforms. This finding led to interest in hIcmt inhibitors as potential anti-cancer agents. Previous analog studies based on N-acetyl-S-farnesylcysteine identified two prenyl-cysteine-based low micromolar inhibitors (1a and 1b) of hIcmt, each bearing a phenoxyphenyl amide modification. In this study, a focused library of analogs of 1a and 1b was synthesized and screened versus hIcmt, delineating structural features important for inhibition. Kinetic characterization of the most potent analogs 1a and 1b established that both inhibitors exhibited mixed-mode inhibition and that the competitive component predominated. Using the Cheng–Prusoff method, the K_i values were determined from the IC_{50} values. Analog 1a has a K_{IC} of 1.4 ± 0.2 μM and a K_{IU} of 4.8 ± 0.5 μM while 1b has a K_{IC} of 0.5 ± 0.07 μM and a K_{IU} of 1.9 ± 0.2 μM. Cellular evaluation of 1b revealed that it alters the sub-cellular localization of GFP-KRas, and also inhibits both Ras activation and Erk phosphorylation in Jurkat cells.

1. Introduction

A target of growing interest in the field of cancer chemotherapeutics is the human protein isoprenylcysteine carboxyl methyltransferase (hIcmt).[1–4] Icmt is the enzyme responsible for the last common step of the posttranslational processing pathway of CaaX proteins.[5,6] The family of CaaX proteins includes many key eukaryotic regulatory proteins, most notably proteins in the Ras family. These proteins terminate with a C-terminal CaaX sequence that is composed of four amino acids in the order of cysteine, followed by two generally aliphatic residues (aa), and a final residue (X) that varies in its identity from protein to protein. The first step of the CaaX protein posttranslational processing pathway is mediated by either protein farnesyl transferase (FTase) or protein geranylgeranyl transferase type I (GGTase-I).[7–9] FTase and GGTase-I respectively attach either a 15-carbon or 20-carbon isoprenoid group to the CaaX cysteine. The type of lipid group added is directed, in part, by the nature of the terminal X residue. Lipidation is followed by proteolytic removal of the –aaX residues by the endoprotease Ras converting enzyme-1 (Rce1).[10] Icmt then carries out the final carboxyl methylation step. Disruption of this pathway via enzyme inhibition prevents Ras proteins from localizing properly in the cell, thereby hindering cellular functionality and obstructing cellular growth.[2,11,12] Therefore, the development of inhibitors of the enzymes in this pathway is desirable for the treatment of cancer driven by oncogenic Ras.

Mutant forms of K-Ras are a frequent cause of several human malignancies, including pancreatic cancers. Research on farnesyl transferase inhibitors (FTIs), once promising cancer chemotherapeutic agents, showed that K-Ras tumors are often resistant to FTI treatment due to alternative geranylgeranylation.[13–16] The reason for this difference lies in the fact that K-Ras can be alternatively geranylgeranylated by GGTase I in the presence of FTIs.[17–19] Although, Icmt recognizes both farnesylated and geranylgeranylated proteins,[20,21] previous studies suggest that the methylation is more important for the proper localization of farnesylated CaaX proteins than for many geranylgeranylated proteins.[20,22]

These data further support that Icmt may prove to be an important target in preventing the function of farnesylated oncogenic Ras proteins, but may not be detrimental to the function of all CaaX proteins. Furthermore, recent studies in cells and mouse models
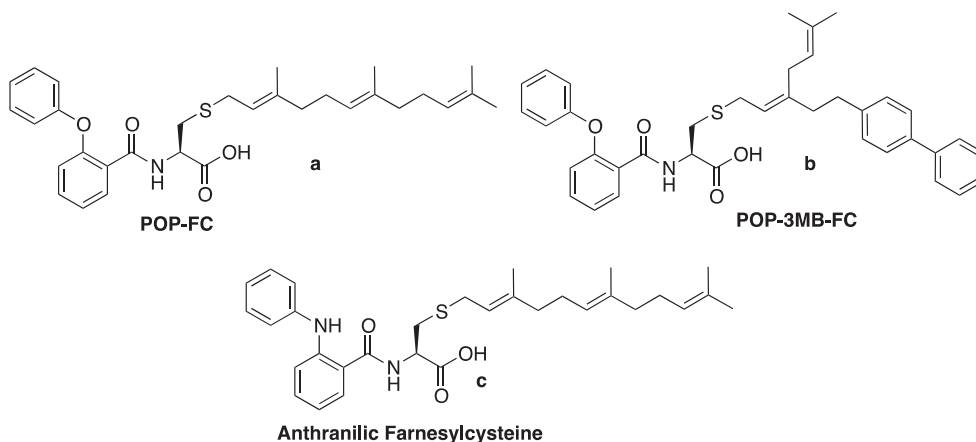
Figure 1. Phenoxyphenyl-farnesylcysteine (**a**, POP-FC), phenoxy-phenyl-3-methylbutenyl-biphenyl farnesylcysteine (**b**, POP-3 MB-FC) and anthranilic farnesylcysteine (**c**).

also support Icmt as a promising chemotherapeutic target.[23,24] Wang et al. have shown that small molecule Icmt inhibitors can induce autophagic cell death in PC3 prostate cancer cells.[23] In mice, inactivation of Icmt has also been shown to inhibit transformation by oncogenic K-Ras and B-Raf.[2] These key findings further support the development of hIcmt inhibitors as chemotherapeutic agents for Ras-driven cancers.

Our laboratories have recently identified 2-phenoxy-phenyl-farnesylcysteine (POP-FC, Fig. 1a) and 2-phenoxyphenyl-3-methylbutenyl-farnesylcysteine (POP-3-MB-FC, Fig. 1b) as lead Icmt inhibitors.[25] These findings prompted us to examine the role of the phenoxy-phenyl motif in achieving Icmt inhibition. The simplest and most widely used amino acid-based Icmt substrate is an amide-modified farnesylated cysteine, N-acetyl-S-farnesylcysteine (AFC).[26–32] The important substrate recognition features of AFC, which mimics the–aaX proteolyzed C-terminus of protein substrates, are the presence of an S-farnesyl moiety, a free α-carboxyl group and an amide modified α-amino group.[26,28] Note that the peptide Icmt substrate LARYK-S-farnesyl-C was found to have a 10-fold lower K_M for mammalian Icmt than AFC,[32] suggesting that the upstream sequence plays a role in recognition and methylation efficiency.

Previous studies from our laboratory have indicated that the human homolog of Icmt may possess an active site that can accommodate substrates or inhibitors with bulky, hydrophobic amide moieties and that certain bulky amide-modified farnesylcysteine (AMFC) analogs can act as low micromolar inhibitors of human Icmt.[25,33,34] In order to further our understanding of the role the

phenoxy-phenyl motif plays in human Icmt (hIcmt) inhibition, a library of compounds was designed and synthesized based on the lead POP-FC (**1a**). Results from this study will help us better understand the role of the phenoxy-phenyl motif in enzyme recognition with the goal of enhancing the potency of these small molecules.

2. Chemistry

The analogs described herein were synthesized using previously established methods in our laboratory.[25,34] The general synthetic design involved utilizing a known synthesis of farnesylcysteine methyl ester[34] and coupling it with the appropriate carboxylic acid using HOBT and HBTU followed by saponification using lithium hydroxide (as shown schematically in Scheme 2).[34] In cases where the carboxylic acid was not commercially available, the appropriate aromatic carboxylic acid was synthesized and coupled to farnesylcysteine methylester.

The structures of the compounds synthesized utilizing this approach are shown in Figure 2. Carboxylic acids needed for the synthesis for compounds **2a–c** and **2e** were commercially available. For compounds **2d** and **2f–h**, each carboxylic acid was synthesized as shown in Scheme 1. The general method involved using an alkoxide anion as the nucleophile to displace a benzylic halide to obtain the respective phenoxy-phenyl analog. The aromatic bromide was then converted into a Grignard reagent using magnesium turnings in THF and quenching the formed Grignard with dry ice. Carboxylic acid **5** used to prepare analog **2d** was synthesized using an Ullmann-type ether coupling as reported previously.[35]
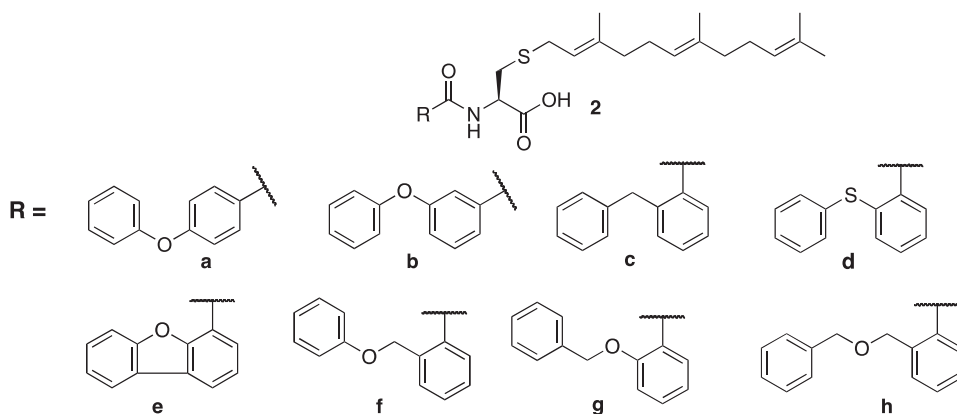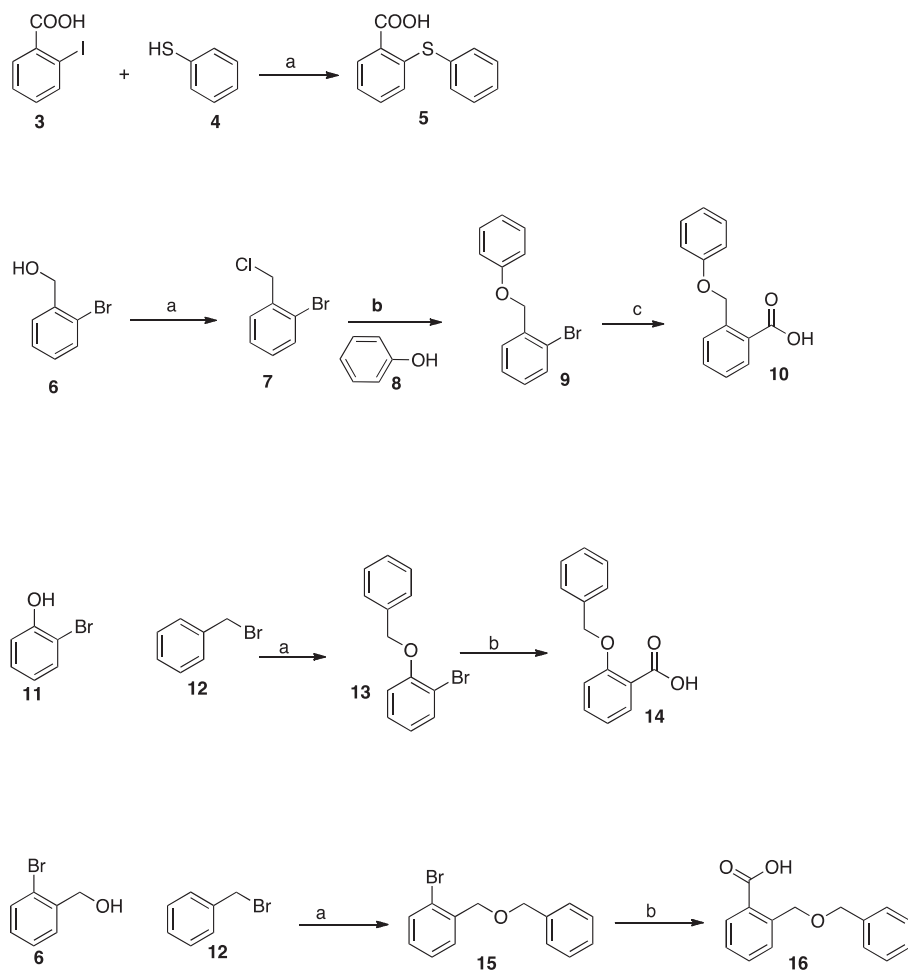

Figure 2. Structures of the phenoxy-phenyl modified analogs synthesized and screened as inhibitors of hIcmt.

Scheme 1. Synthesis of various carboxylic acids. Reagents and conditions: (a) Synthesis of 2-(phenylthio)benzoic acid: (a) Potassium hydroxide, 5 equiv; Cu powder, 0.1 equiv; water (86%); (b) Synthesis of 2-(phenoxymethyl)benzoic acid: (a) NCS, dimethylsulfide, DCM, 73%, (b) NaH, DMF, 0 °C to rt, 4 h, 62%, (c) Mg turnings, 1,2 dibromoethane, CO_2 quench, then 10% HCl, 68%.; (c) Synthesis of 2-(benzyloxy)benzoic acid: (a) NaH, DMF, 0 °C to rt, 4 h, 67% (b) Mg turnings, 1,2 dibromoethane, CO_2 quench, then 10% HCl 78%.; (d) Synthesis of 2-((benzyloxy)methyl)benzoic acid: (a) NaH, DMF, 0 °C to rt, 4 h, 77% (b) Mg turnings, 1,2 dibromoethane, CO_2 quench, then 10% HCl, 45%.
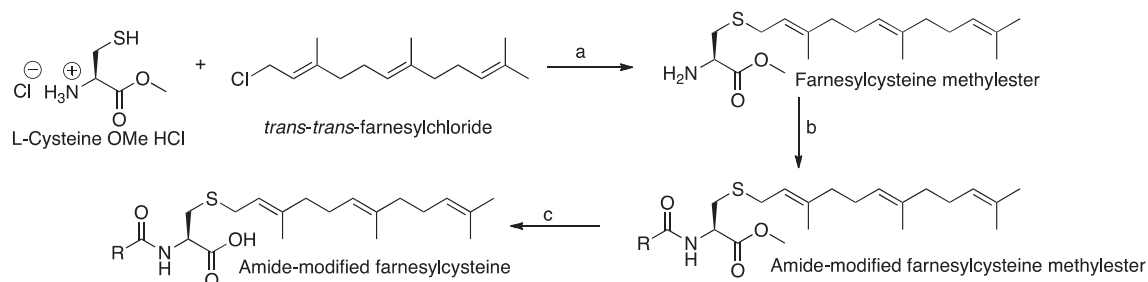
Scheme 2. General synthetic scheme showing synthesis of analogs **2a–2h**. (a) 7N NH_3 in methanol, 0 °C, 3 h, 80%; (b) HOBT, HBTU, DIEA, DMF, 0 °C to rt, 6–10 h, 48–93% (c) LiOH in methanol, 2 h, 60–85%.

We also designed and synthesized molecules in which the phenoxyphenyl amide scaffold was maintained but the prenyl chain was modified. To this end, we synthesized analogs **17–21** shown in Figure 3. Their synthesis is depicted in Schemes 3 and 4. Analog **17** is the enantiomer of our lead **1a**, while analogs **18** and **19** contain a shorter geranyl (10 carbon) and a longer geranyl-geranyl (20 carbon) chain, respectively. Analog **20** (synthesis shown in Scheme 4) was specifically designed to investigate the role of the amide proton in hIcmt inhibition and analog **21**, with an undecyl moiety was designed to probe the importance of the

prenyl chain in achieving hIcmt inhibition. We have recently reported that a similar change from prenyl to straight chain alkyl is detrimental to hIcmt inhibition when the amide linkage was replaced with a sulfonamide bond.[36] We wanted to investigate whether such a change is consistent across different classes of inhibitors. The N-methyl analog **20** was synthesized using a solid-phase methodology using the advanced intermediate **23**, which was synthesized as reported previously.[37] Compound **23** was loaded on the 2-chlorotrityl-chloride resin, which is essential to this synthesis due to the acid sensitivity of the prenyl chain. After
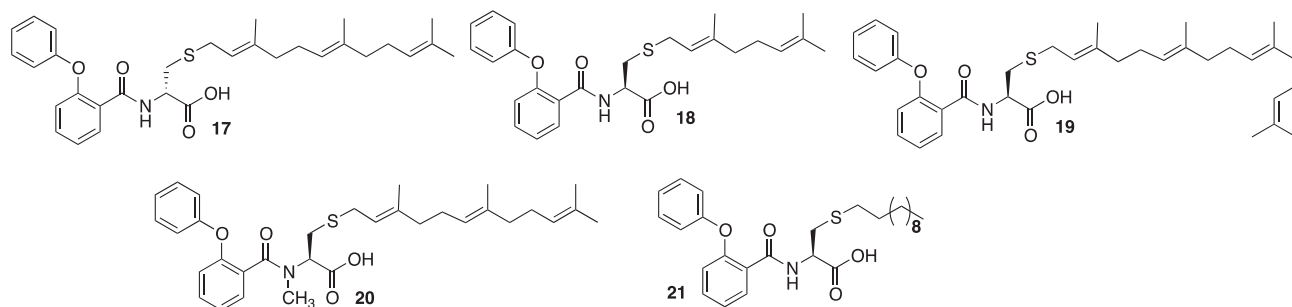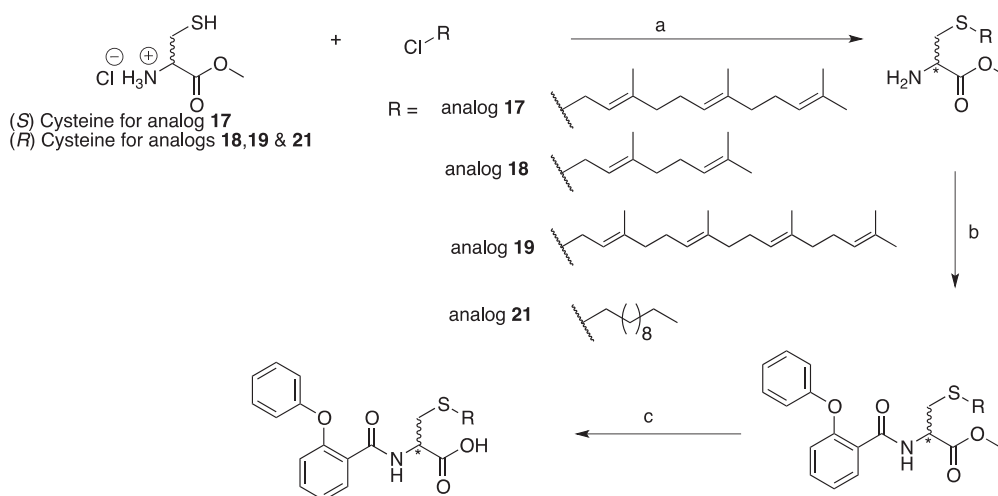
Figure 3. Structures of the phenoxy-phenyl prenyl modified analogs synthesized and screened as inhibitors of hIcmt.

Scheme 3. Synthesis of prenyl-modified phenoxy-phenyl analogs. Reagents and conditions: (a) 7 N NH$_3$ in Methanol, 0 °C, 3–12 h, 66–80% (b) HOBT, HBTU, DIEA, DMF, 0 °C to rt, 6–10 h, 48–93% (c) LiOH in methanol, 2 h, 60–85%.

loading, the disulfide-protecting group was removed using DTT and the farnesyl group was attached to the free thiol using farnesyl chloride. The 2-phenoxyphenyl carboxylic acid was then coupled to the secondary amine using standard coupling procedures previously used in our laboratory.[25] Compound **20** was obtained upon cleavage from the resin using 0.2% TFA in DCM. Following their syntheses, the compounds were evaluated as substrates and inhibitors of hIcmt using a vapor diffusion assay.[5,38,39]

## 3. Results and discussion

3.1. In vitro biochemical evaluation of analogs

Analogs **2a–h** and **17–21** were first tested as substrates for hIcmt at 25 μM as described in the experimental section. Upon evaluation, none of the analogs showed substrate activity (data not shown). The compounds were subsequently tested as inhibitors at 10 μM in the presence of 25 μM of the substrate AFC and all the analogs were inhibitors of hIcmt to varying degrees. Compounds **2a** and **2b** were specifically synthesized and tested to evaluate the importance of the positioning of the phenoxy-phenyl motif in hIcmt inhibition. Both of these analogs were poor inhibitors of hIcmt, both inhibiting hIcmt by less than 30% at 10 μM. We experimentally determined the IC$_{50}$ of compound **2b** to be 22.6 ± 1.2 μM. This value reflects an approximately five-fold loss in activity between the ortho and para isomers of the phenoxy-phenyl motif, suggesting that the ortho-phenoxyphenyl motif is important for hIcmt inhibition. Note that the para regio-isomer is a significantly poorer inhibitor compared to both the meta and the ortho isomer.

We have previously reported the synthesis of the anthranilic acid analog (Fig. 1c), where the phenoxy-phenyl oxygen is replaced by a nitrogen atom.[25] This compound has an IC$_{50}$ of 7.1 μM against hIcmt. Although less potent than the parent compound **1a**, the less electronegative nitrogen does not result in a significant loss of activity. We next wanted to evaluate the effect of changing the size and electronegativity of the central atom connecting the ortho-substituted phenyl ring. To this end, we synthesized analogs **2c** and **2d**. The decreased electronegativity of the carbon and sulfur atom linkers resulted in a roughly fourfold loss of inhibitory activity as compared to compound **1**a, suggesting that the electronegativity of the connecting atom between the two-phenyl rings may be a determining factor for inhibitory activity. More electronegative atoms such as oxygen and nitrogen present in the structure resulted in better inhibitors than those containing less electronegative atoms such as carbon and sulfur.

The biochemical evaluation described above suggested that the ortho substituted phenoxy-phenyl motif was important for hIcmt inhibition. To further investigate the effect of the spatial orientation of the oxygen connector atom and the second phenyl ring on hIcmt inhibition, we synthesized and evaluated analogs **2e**–**2h**. Conformational restriction of the two phenyl rings through a dibenzofuran scaffold (compound **2e**) diminished inhibitory activity significantly, as did replacing the central one oxygen linker with a two-atom linker in analogs **2f** and **2g**. It is worth noting that analog **2g**, which retains the position of the oxygen atom relative to the amide bond, displays much greater inhibition as compared to analog **2f**. The inhibitory effect of analog **1a** could result from the two oxygen atoms' (the amide carbonyl oxygen and the linker oxygen), involvement in a critical interaction because increasing
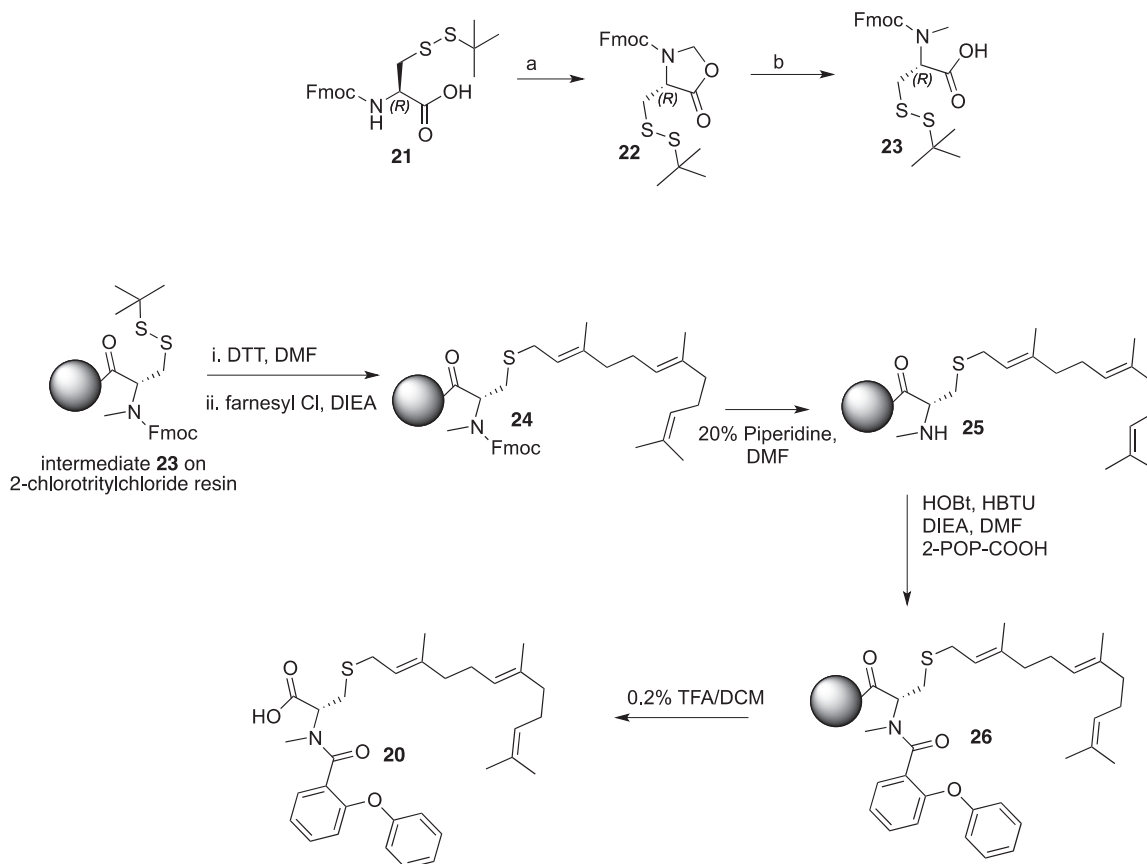
Scheme 4. Synthesis of *N*-methyl POP-FC. (a) Benzene, (HCHo)*n*, PTSA, reflux, 10 h; (b) TES,TFA.

the distance between those two oxygen atoms reduced the inhibitory potency of the molecule. Analog **2h**, where the central oxygen linker is more flexible compared to **1a** is a poor inhibitor compared to compound **1a**.

To evaluate the effect of the stereochemistry of the amino acid derivative POP (**1a**) on hIcmt inhibition, we synthesized its enantiomer (**17**). We have recently demonstrated that the stereochemistry at the alpha carbon is not critical for hIcmt inhibition in a sulfonamide series[36] and consistent with this result, analog **17** inhibited hIcmt with an IC$_{50}$ of 7.8 ± 0.4 μM, nearly equivalent to **1a**, which demonstrated an IC$_{50}$ of 6.2 ± 0.7 μM. Next, to interrogate the importance of the farnesyl chain in analog **1a**, we synthesized analogs **18**, **19** and **21**. The farnesyl group appears to be very important to hIcmt inhibition because the short and longer prenyl analogs **18** and **19** exhibited significant loss of hIcmt inhibition at 10 μM. The undecyl analog, **21**, was a particularly poor inhibitor of hIcmt at the test concentration. These data suggest that the presence of a farnesyl chain on the cysteine sulfur is a critical pharmacophore for hIcmt inhibition. These data corroborate our previous findings about the importance of the farnesyl chain for hIcmt inhibition.[33,36] Finally, to interrogate the effect of the amide proton on hIcmt inhibition, we synthesized analog **20** using the solid-phase strategy described above. This analog was equivalent to our previous lead, **1a**, in terms of percent inhibition of hIcmt activity and has a similar IC$_{50}$ of 6.7 ± 0.4 μM. The presence of a methyl group on the amide nitrogen appears to have minimal effect on the inhibition potential of the analog, suggesting that the amide region of the molecule may be no more important than serving as a linker between the phenoxy-phenyl and the farnesyl moieties (Table 1).

Overall, our biochemical data suggest that the *ortho*-phenoxy-phenyl motif is important and replacement with other regioisomers leads to a significant decrease in potency. The presence and the position of the oxygen atom connecting the two phenyl rings are also important features, as any change in the atom itself or its spatial positioning reduces hIcmt inhibition. Stereochemistry about the alpha carbon of cysteine and the amide proton both appear inconsequential to hIcmt inhibition. The most important element in hIcmt inhibition with this class of compounds is the farnesyl chain itself, as any deviation from the 15-carbon isoprene results in a loss of inhibition, which is particularly evident with the undecyl analog **21**, a very poor hIcmt inhibitor.

3.2. Kinetic mode of inhibition for compounds 1a and 1b

In order to determine the mode of inhibition of hIcmt by compounds **1a** and **1b**, the most potent inhibitors in this series of compounds, kinetic assays were performed in which the small molecule substrate (AFC) concentration was varied while the inhibitor concentration remained fixed. The data for each inhibitor concentration were averaged from three trials, and plotted as double reciprocal plots (Fig. 4 and 5). These inhibitors displayed mixed-type inhibition in which the competitive component dominated, as demonstrated by an α value greater than 1.[52] K_i Values for compounds **1a** and **1b** were then determined from the IC$_{50}$ values using the Cheng–Prusoff method as adapted by Cer et al.[53] For compound **1a**, the competitive (K_{IC}) and uncompetitive (K_{IU}) values were 1.4 ± 0.2 μM and 4.8 ± 0.5 μM, respectively. For compound **1b**, the K_{IC} and K_{IU} values were 0.5 ± 0.07 μM and K_{IU} 1.9 ± 0.2 μM, respectively.

Table 1
Inhibition profiles of the analogs

Structure	Analog	IC$_{50}$[a,b] (µM)
	AFC (negative control)	NA
	1a (POP-FC–pos. control)	6.2 ± 0.7[a]
	1b (POP-3MB-FC)–pos. control	2.5 ± 0.3[a]
	2a	63[b]
	2b	22.6 ± 1.2[a]
	2c	38[b]
	2d	14.7 ± 0.8[a]
	2e	58[b]
	2f	75[b]
	2g	13.4 ± 0.6[a]
	2h	49[b]
	17	7.8 ± 0.4[a]
	18	149[b]
	19	38[b]

Table 1 (continued)

Structure	Analog	IC$_{50}$[a,b] (µM)
	20	6.7 ± 0.4[a]
	21	210[b]

[a] IC$_{50}$ values are mean of three experiments, were determined using the vapor diffusion assay and calculated using GRAPH-PAD PRISM 5.0. Concentration of the substrate used (AFC) was 25 µM.

[b] Estimated IC$_{50}$ values obtained using an in-house equation ($y = -26.813x + 77.293$; where y = percent inhibition at 10 µM and $x = \log[\text{IC}_{50}]$) that correlates percent inhibition value at 10 µM inhibitor concentration (in presence of 25 µM substrate, AFC, concentration) to experimental IC$_{50}$ values. This logarithmic correlation has a $R^2 = 0.85$.
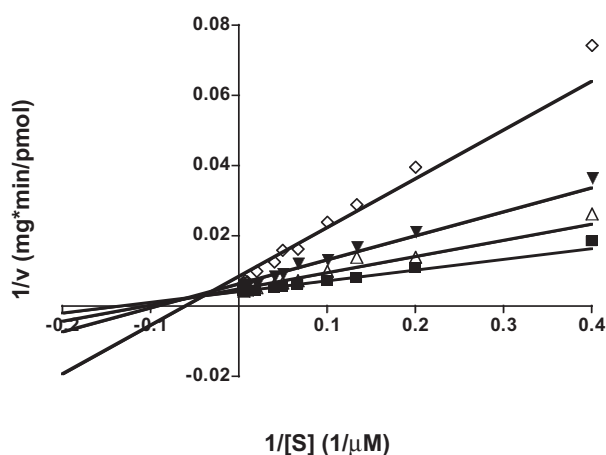

Figure 4. Mode of inhibition and K_i determination of compound **1a**. 1a Displays mixed-type inhibition. Lineweaver–Burk plots illustrate the mode (mixed) of inhibition of hIcmt by **1a**. These are double reciprocal plots from AFC substrate curves with hIcmt, in the presence of the indicated concentration of inhibitor, which were obtained as described in Section 6.2. The K_{IC} is 2.6 ± 0.5 µM and the K_{IU} is 10.5 ± 1.4 µM.

Figure 5. Mode of inhibition and K_i determination of compound **1b**. The phenoxyphenyl analog, **1a**, demonstrated mixed-type inhibition with a K_{IC} of 1.2 ± 0.2 µM and a K_{IU} of 11.2 ± 2.4 µM. Lineweaver–Burk plots were obtained by the same method as that described for Figure 4.

4. Cellular effects of Icmt inhibitor 1b

4.1. Pop-3MB (1b) alters the subcellular localization of GFP-K-Ras in Jurkat T cells

Proper posttranslational processing is a prerequisite for Ras membrane localization and function. To determine the cellular effects of our most potent inhibitor **1b**, the membrane localization of fluorescently tagged K-Ras was visualized in the presence and absence of **1b**.[40,41] We transfected Jurkat T cells with GFP-K-Ras and treated the cells with delivery vehicle alone, the statin drug simvastatin (which blocks K-Ras prenylation), or **1b**. The cells were fixed and GFP-K-Ras localization was visualized using fluorescent microscopy. After 24 h of treatment, GFP-K-ras localization was categorized into three groups: normal plasma membrane localization, partial mislocalization, and complete mislocalization. This was determined via visual inspection of randomly selected fields containing 100 cells. Representative examples of normal, partial and complete mislocalization are shown in Figure 6b (determined as described in the Section 6). The results demonstrated that 0.1 µM **1b** prevented approximately 35% protein membrane localization while treatment with 10 µM compound **1b** prevented 75% of membrane localization (Fig. 6a and b). These data suggest that **1b** is taken up into mammalian cells and functions as an Icmt
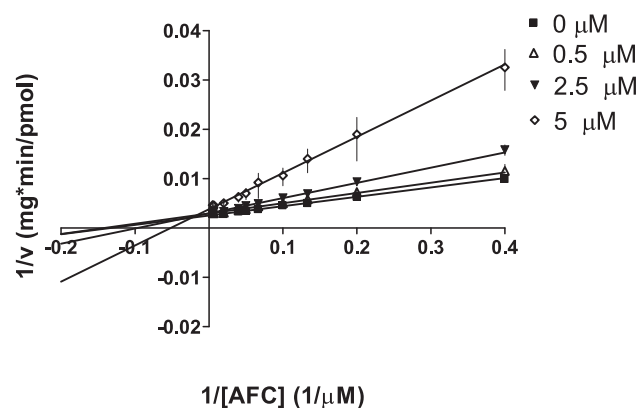
inhibitor, preventing K-Ras membrane localization. Surprisingly, the data indicate that significant cellular mislocalization of GFP-K-Ras is seen at compound levels that are significantly lower than the biochemical IC$_{50}$ value for **1b**. While we are unclear as to the reason for this result, there are at least two possibilities. First, this compound may preferentially accumulate in Jurkat cells. Alternatively, this compound may, in addition to inhibiting Icmt, block GFP-K-Ras through another mechanism, possibly related to that proposed for Salirasib by Kloog and co-workers.[45–47]

4.2. Pop-3MB (1b) inhibits Erk phosphorylation and Ras activation in Jurkat T cells

Low-grade stimulation through the T-cell receptor (TCR) in Jurkat cells results in Ras dependent Erk activation.[42] We therefore utilized signaling assays with low grade TCR stimulation to evaluate the effects of **1b** on Erk and Ras activation. Cells were treated with delivery vehicle (DMSO), simvastatin, or **1b**. After 24-hour vehicle or drug treatment, Jurkat cells were low-grade stimulated through the TCR with anti-CD-3ε to activate the Ras-MAPK-Erk pathway. To test Ras activation, the stimulated cells were lysed and active GTP-bound Ras was precipitated from whole cell lysates using a GST-RBD (Ras Binding Domain) pulldown assay.[43] As shown in Figure 7b, compound **1b** decreased Erk activation approximately three-fold compared to the control. Furthermore, **1b** also inhibited Ras activation significantly as seen in Figure 7c. These data suggest that the alterations in TCR-dependent Erk
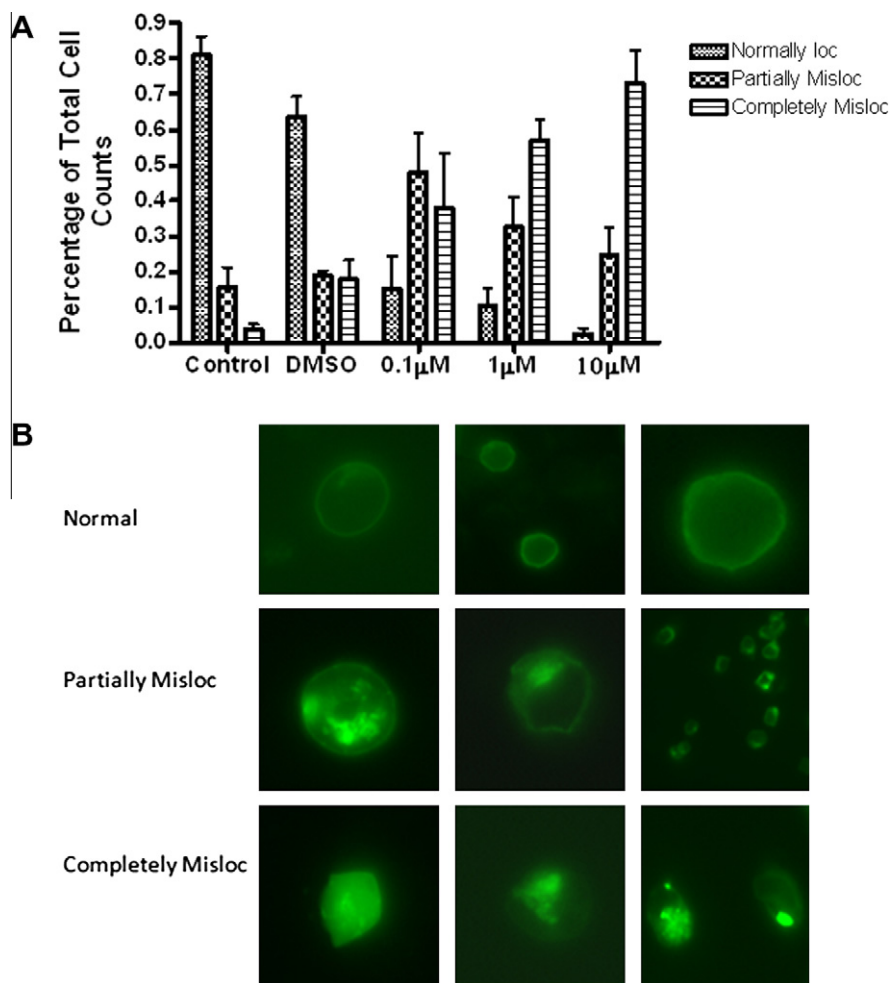
Figure 6. Compound **1b** alters the subcellular localization of GFP K-Ras in Jurkat T cells. Jurkat T cells were transiently transfected with GFP-K-Ras and treated with DMSO or **1b** at indicated concentrations for 24 h. (A) Histograms depict the differences in GFP-K-Ras localization after indicated treatments. Differences were defined as partial or complete loss of normal localization, as defined by the images shown in (B). Results are representative of three independent experiments.

phosphorylation and Ras activation in Jurkat T cells are due to the inhibition of Ras methylation by compound **1b**.

5. Conclusion

We have demonstrated that low-micromolar inhibitors of hIcmt alter the sub-cellular location of GFP-Ras and also have an effect in the downstream pathway. Inhibition of anti-CD-3ε dependent Erk phosphorylation and Ras activation in Jurkat T cells by compound **1b** suggests that hIcmt inhibitors hold promise in treatment of K-Ras driven cancers. Our SAR data with the entire series of compounds reported here have provided insight into the potential pharmacophoric requirements for hIcmt inhibition. As there is yet no three-dimensional structural information for hIcmt, given that it is an integral membrane protein, these data generated from our compounds are a small step forward in understanding the inhibition requirements for hIcmt. Stereochemistry at the alpha carbon has no significant bearing on the outcome for inhibition. Our data further suggest that the farnesyl chain is the most important scaffold for substrate-based Icmt inhibitors and any change in length or overall hydrophobicity decreases inhibition. Cysmethynil, a small molecule inhibitor of Icmt[44] has demonstrated induction of autophagic cell death in PC3 prostate cancer cells,[23] and thus has shown promise for cancer therapy. Salirasib, a partial inhibitor of Icmt has also shown promise in phase I clinical trials.[45–47] In contrast, a recent report demonstrated that very potent

Icmt inhibitors reduced cell viability only modestly in several cancer cell lines.[48] These reports, coupled with our results published here suggest that Icmt inhibitors have utility in treating Ras-driven cancers. Further studies with substrate-based hIcmt inhibitors, such as those developed in our laboratory, will help to clarify the therapeutic potential of hIcmt inhibition. Analog **1b** is a promising lead and suggests that appropriate prenyl mimics can be developed to achieve potent hIcmt inhibition and efforts are currently underway to exploit these findings.

6. Experimental

6.1. Synthesis and spectral analysis

General Procedure for the synthesis of analogs **2a–2h**

6.1.1. Synthesis of farnesylcysteine methylester

L-Cysteine methylester hydrochloride (1.0 equiv) (obtained from Sigma–Aldrich) was charged to a dry round bottom flask and the atmosphere inside the flask was replaced with argon. The reaction mixture was maintained at 0 °C and 5 mL of 7 N ammonia in methanol (purchased from Sigma–Aldrich) was added to the L-cysteine methylester hydrochloride. The contents were allowed to stir for 15 min following which, *trans–trans*-farnesylchloride (0.95 equiv) (purchased from Sigma–Aldrich) was syringed into the flask. The reactants were allowed to react for 3 h at 0 °C.
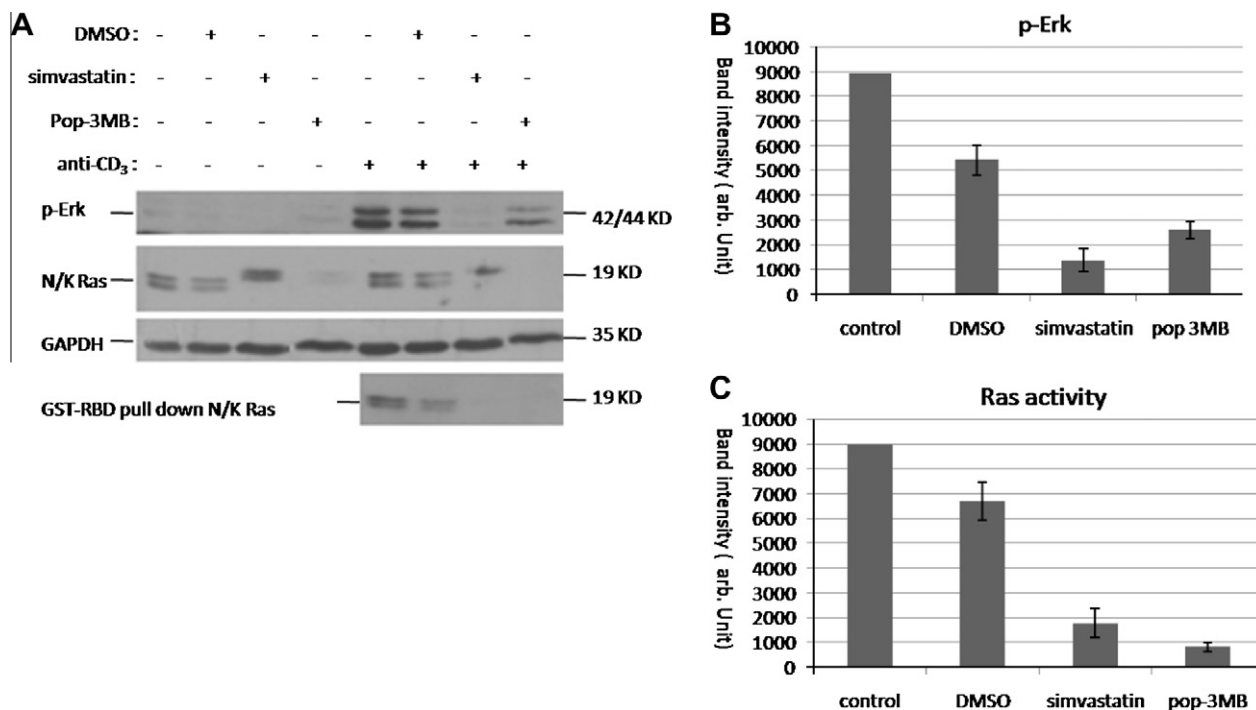
Figure 7. Inhibition of anti-CD-3ε dependent Erk phosphorylation and Ras activation in Jurkat T cells following **1b** treatment (25 μM). Jurkat T cells were treated with vehicle, simvastatin (36.7 μM) or **1b** for 24 h followed by stimulation with anti-CD-3ε (20 μg/mL) (A) The phosphorylation of Erk was detected by immunoblotting the cell lysate with an anti-phospho-Erk antibody (top). The active form of Ras was precipitated from the cell lysate with a GST-RBD fusion protein. Precipitated Ras was detected by immunoblotting using an anti-pan-Ras antibody (bottom). Immunodetection of GAPDH was used as the loading control. Erk phosphorylation (B) and Ras activation (C) were quantified using ImageJ (NIH). The results are representative of three independent experiments.

The reaction was monitored by TLC analysis. The contents of the round bottom flask were evaporated to dryness and purified by column chromatography via isocratic elution using a mixture of methanol and dichloromethane (1:9). This yielded farnesylcysteine methylester in 80% yield. The spectral data matched the reported data.[34,49]

6.1.2. Synthesis of the amide-modified farnesylcysteine methylester intermediate

The appropriate carboxylic acid (1.0 equiv) was charged to a dry round bottom flask and was dissolved in dimethylformamide (DMF). Diisopropylethylamine (1.1 equiv), HOBT (1.1 equiv) and HBTU (1.1 equiv) were added to this and the contents were allowed to react at 0 °C for 30 min. This was followed by addition of a solution of farnesylcysteine methylester in DMF. The contents were allowed to react for 2 h. The reaction was monitored by TLC analysis. On completion of the reaction, 10% aqueous citric acid was added to the reaction mixture and the product was extracted using ethylacetate (20 mL) as the solvent. The solvent was removed under vacuum utilizing a rotary evaporator and the residue was loaded on a short (2–3 inches) silica gel plug. The silica gel plug was flushed with 3% methanol in dichloromethane to obtain the crude coupling product.

6.1.3. Synthesis of the amide-modified farnesylcysteine (free acid)

The crude product obtained from the previous step was dissolved in methanol and was transferred to a round-bottom flask. The contents were allowed to cool to 0 °C. Lithium hydroxide (1.1 equiv) was added to the mixture and the contents were allowed to react for 2 h. Following the completion of the reaction, the solvent was removed under reduced pressure and the mixture was loaded on a silica gel column. Chromatographic separation was performed under the influence of gravity using a 1:9 mixture of methanol and methylenechloride.

6.1.3.1. Compound 2a: (R)-2-(4-Phenoxybenzamido)-3-(((2E, 6E)-3,7,11-trimethyldodeca-2,6,10-trien-1-yl)thio)propanoic acid.
^{1}H NMR (300 MHz, CDCl$_3$) δ 7.80 (m, 3H), 7.33 (dd, J = 18.3, 10.6 Hz, 2H), 7.06 (m, 4H), 5.41–4.74 (m, 4H), 3.13 (m, 4H), 2.10–1.87 (m, 8H), 1.67 (d, J = 6.5 Hz, 3H), 1.59 (d, J = 4.5 Hz, 3H), 1.56 (s, 3H). ^{13}C NMR (75 MHz, CDCl$_3$) δ 176.81, 135.09, 134.77, 131.17, 131.06, 129.86, 124.31, 124.03, 123.81, 119.74, 117.51, 39.66, 39.56, 26.69, 26.48, 25.70, 25.66, 25.63, 17.65, 17.59, 16.08, 15.95, 15.79.

6.1.3.2. Compound 2b: (R)-2-(3-Phenoxybenzamido)-3-(((2E, 6E)-3,7,11-trimethyldodeca-2,6,10-trien-1-yl)thio)propanoic acid.
^{1}H NMR (300 MHz, CDCl$_3$) δ 8.03–7.68 (m, 4H), 7.67–7.46 (m, 3H), 7.37 (t, J = 7.2 Hz, 1H), 7.20 (d, J = 18.4 Hz, 1H), 5.38 (dd, J = 13.7, 7.3 Hz, 3H), 4.98 (d, J = 29.8 Hz, 1H), 3.61–2.94 (m, 4H), 2.48–2.08 (m, 8H), 1.94 (d, J = 14.1 Hz, 3H), 1.88 (s, 3H), 1.85 (s, 6H). ^{13}C NMR (75 MHz, CDCl$_3$) δ 176.38, 167.17, 157.37, 156.40, 139.73, 135.21, 135.05, 131.12, 129.73, 124.26, 124.22, 123.76, 123.57, 121.85, 121.50, 119.32, 119.07, 117.94, 53.49, 39.61, 39.51, 29.98, 26.64, 26.43, 25.62, 25.59, 17.61, 16.01, 15.91.

6.1.3.3. Compound 2c: (R)-2-(2-Benzylbenzamido)-3-(((2E,6E)-3,7,11-trimethyldodeca-2,6,10-trien-1-yl)thio)propanoic acid.
^{1}H NMR (300 MHz, MeOH) δ 7.32 (d, J = 6.7 Hz, 1H), 7.18–6.89 (m, 8H), 5.05 (t, J = 7.4 Hz, 1H), 4.92 (t, J = 6.3 Hz, 2H), 4.51 (s, 1H), 4.13–3.93 (m, 2H), 3.11–2.99 (m, 2H), 2.78 (ddd, J = 22.1, 13.6, 5.6 Hz, 2H), 1.98–1.72 (m, 8H), 1.50 (d, J = 4.1 Hz, 6H), 1.42 (s, 6H). ^{13}C NMR (75 MHz, MeOH) δ 172.60, 160.82, 142.20, 140.57, 140.30, 137.60, 136.13, 132.03, 131.45, 131.01, 130.28, 129.36, 128.46, 127.10, 127.01, 125.43, 125.11, 121.51, 40.83, 40.71, 27.77, 27.42, 25.98, 17.85, 16.35, 16.21.

6.1.3.4. Compound 2d: (R)-2-(2-(Phenylthio)benzamido)-3-(((2E,6E)-3,7,11-trimethyldodeca-2,6,10-trien-1-yl)thio)propanoic acid. ^{1}H NMR (300 MHz, CDCl₃) δ 7.61 (d, J = 32.1 Hz, 1H), 7.37 (s, 3H), 7.28 (d, J = 3.6 Hz, 3H), 7.14 (s, 2H), 7.01 (s, 1H), 5.23–4.93 (m, 3H), 4.80 (s, 1H), 3.12 (s, 2H), 2.93 (t, J = 28.2 Hz, 2H), 1.99 (dd, J = 17.7, 6.9 Hz, 8H), 1.67 (s, 3H), 1.59 (s, 5H), 1.55 (s, 3H). ^{13}C NMR (75 MHz, CDCl₃) δ 171.57, 168.04, 139.63, 136.60, 135.04, 133.98, 133.09, 131.15, 130.88, 129.32, 128.84, 127.92, 126.13, 124.27, 123.81, 119.51, 77.42, 77.00, 76.57, 58.58, 39.62, 39.53, 33.17, 30.02, 26.65, 26.46, 25.65, 17.64, 16.13, 15.95.

6.1.3.5. Compound 2e: (R)-2-(Dibenzo[b,d]furan-4-carboxamido)-3-(((2E,6E)-3,7,11-trimethyldodeca-2,6,10-trien-1-yl)thio)-propanoic acid. ^{1}H NMR (300 MHz, CDCl₃) δ 8.56 (s, 1H), 8.09 (d, J = 17.2 Hz, 1H), 7.85–7.42 (m, 3H), 7.35 (s, 1H), 7.22 (s, 2H), 5.15 (s, 1H), 5.09–4.81 (m, 3H), 3.38–3.04 (m, 4H), 1.94 (dd, J = 19.0, 7.0 Hz, 8H), 1.64 (s, 3H), 1.56 (s, 3H), 1.47 (d, J = 12.5 Hz, 5H). ^{13}C NMR (75 MHz, CDCl₃) δ 176.57, 168.75, 156.31, 152.11, 140.64, 136.04, 132.16, 129.75, 128.50, 125.29, 124.77, 124.21, 123.82, 121.35, 120.57, 112.87, 61.28, 40.60, 40.49, 34.29, 31.15, 27.65, 27.39, 26.64, 18.63, 17.00, 16.89, 12.33.

6.1.3.6. Compound 2f: (R)-2-(2-(Phenoxymethyl)benzamido)-3-(((2E,6E)-3,7,11-trimethyldodeca-2,6,10-trien-1-yl)thio)prop-anoic acid. ^{1}H NMR (300 MHz, CDCl₃) δ 7.61 (s, 1H), 7.47 (d, J = 6.6 Hz, 2H), 7.30 (d, J = 17.7 Hz, 1H), 7.21 (t, J = 7.0 Hz, 3H), 6.91 (dd, J = 20.5, 7.4 Hz, 3H), 5.34–4.92 (m, 5H), 4.61 (s, 1H), 2.97 (s, 3H), 2.62 (s, 1H), 2.10–1.79 (m, 8H), 1.68 (s, 3H), 1.60 (s, 3H), 1.55 (s, 3H), 1.51 (s, 3H).

6.1.3.7. Compound 2g. ^{1}H NMR (300 MHz, CDCl₃) δ 8.72 (d, J = 7.2 Hz, 1H), 8.22 (dd, J = 7.8, 1.6 Hz, 1H), 7.50 (d, J = 6.5 Hz, 2H), 7.46–7.29 (m, 4H), 7.13–6.98 (m, 2H), 5.26 (d, J = 10.5 Hz, 2H), 5.10 (d, J = 18.0 Hz, 3H), 4.94 (dd, J = 12.1, 6.7 Hz, 1H), 3.08 (ddd, J = 20.4, 13.2, 7.8 Hz, 3H), 2.79 (ddd, J = 20.5, 13.9, 7.8 Hz, 2H), 2.05–1.90 (m, 8H), 1.67 (s, 3H), 1.62–1.57 (m, 9H). ^{13}C NMR (75 MHz, CDCl₃) δ 175.33, 164.65, 156.96, 139.67, 135.43, 135.19, 133.04, 132.37, 131.20, 129.17, 128.49, 127.99, 124.33, 123.68, 121.39, 120.94, 119.57, 112.68, 77.43, 77.00, 76.58, 71.22, 52.44, 52.29, 39.61, 39.53, 32.90, 29.68, 26.63, 26.34, 25.62, 17.62, 16.01, 15.93.

6.1.3.8. Compound 2h: (R)-2-(2-((Benzyloxy)methyl)benzamido)-3-(((2E,6E)-3,7,11-trimethyldodeca-2,6,10-trien-1-yl)-thio)propanoic acid. ^{1}H NMR (300 MHz, CDCl₃) δ 8.10 (d, J = 6.8 Hz, 1H), 7.71 (t, J = 8.2 Hz, 1H), 7.36 (dd, J = 11.4, 4.5 Hz, 2H), 7.33–7.29 (m, 4H), 7.27 (d, J = 3.7 Hz, 1H), 5.19–4.99 (m, 3H), 4.66 (d, J = 11.3 Hz, 1H), 3.36 (s, 4H), 3.07 (dd, J = 12.5, 7.4 Hz, 2H), 2.87–2.71 (m, 2H), 2.11–1.88 (m, 8H), 1.65 (d, J = 12.1 Hz, 3H), 1.58 (s, 6H), 1.56 (s, 3H). ^{13}C NMR (75 MHz, CDCl₃) δ 175.72, 170.17, 140.64, 138.58, 136.17, 136.09, 132.14, 131.54, 131.21, 130.05, 129.28, 129.22, 128.65, 128.59, 125.21, 124.69, 120.37, 73.07, 71.12, 51.07, 40.57, 40.47, 34.25, 30.78, 27.60, 27.36, 26.58, 18.57, 16.97, 16.87.

6.1.4. Synthesis of compound 5

To a solution of potassium hydroxide (5.0 equiv) in water were added 2-iodobenzoic acid (1.0 equiv), thiophenol (1.0 equiv) and Copper powder (0.1 equiv). The contents were refluxed for 12 h, cooled to room temperature and acidified with 4 N hydrochloric acid. Acidification resulted in precipitation of product.

6.1.4.1. Compound 5: 2-(Phenylthio)benzoic acid. ^{1}H NMR (300 MHz, CDCl₃) δ 7.85 (dd, J = 7.8, 1.4 Hz, 1H), 7.37–7.27 (m, 2H), 7.24–7.12 (m, 3H), 7.02–6.95 (m, 1H), 6.87 (dd, J = 10.9, 4.2 Hz, 1H), 6.52 (d, J = 8.1 Hz, 1H). ^{13}C NMR (75 MHz, CDCl₃) δ

172.50, 145.62, 136.84, 134.13, 133.11, 133.00, 130.81, 130.30, 128.12, 126.19, 125.24.

6.1.4.2. General synthetic methodology for bromides 9, 13 and 15. In general, phenol (1.0 equiv) (or the corresponding benzyl alcohol) was charged to a dry round-bottom flask and anhydrous DMF was added to it. The atmosphere in the flask was replaced with argon. Upon complete dissolution of the phenol (or the benzyl alcohol), the contents were cooled to 0 °C and allowed to stir for 15 min. This was followed by addition of sodium hydride (1.1 equiv) and the compounds were allowed to react for one hour. Following this time period, a solution of the appropriate benzyl bromide (1.2 equiv) was added as a solution in anhydrous DMF over a period of 10 min. The contents were allowed to react for 3 h. The reaction was quenched with ice and the product was extracted with ether, followed by washing with 10% citric acid (3 × 20 mL), then washed with 2 M NaOH (to remove the unreacted phenol) and brine. The organic fractions were pooled and concentrated under vacuum to yield product. A chromatographic separation was performed using 2:8 ethylacetate and hexanes if it was necessary.

6.1.4.3. General procedure for synthesis of carboxylic acids 10, 14 and 16. Magnesium turnings (4.0 equiv) were placed in a dry round bottom flask and flame-dried under a steady stream of argon. Upon cooling of the flask to room temperature, anhydrous THF and one drop of 1,2-dibromoethane were added to the flask. The contents were allowed to react for 5 min followed by addition of the appropriate bromide (as a solution in anhydrous THF) over a period of 5 min. The Grignard reagent was allowed to form for 2.5 h and was quenched with dry ice. This was followed by addition of 10% hydrochloric acid (10 mL). The contents from the reaction quench were transferred to a separatory funnel, followed by addition of ethylacetate (20 mL). The aqueous phase was extracted with ethylacetate (3 × 20 mL). The combined organic extracts were treated with 5% sodium hydroxide (3 × 5 mL). Concentrated hydrochloric acid was added to the combined aqueous phase until the pH of the solution was 2.5, which resulted in the precipitation of the product. Filtration of the precipitate yielded the desired carboxylic acid in 45–78% yields.

6.1.4.4. Compound 9: 1-Bromo-2-(phenoxymethyl)benzene. ^{1}H NMR (300 MHz, CDCl₃) δ 7.71 (d, J = 8.0 Hz, 2H), 7.45 (dt, J = 7.6, 6.4 Hz, 3H), 7.29 (dd, J = 12.1, 4.4 Hz, 1H), 7.14 (t, J = 8.1 Hz, 3H), 5.27 (s, 2H). ^{13}C NMR (75 MHz, CDCl₃) δ 159.27, 137.20, 133.40, 130.41, 130.01, 129.69, 128.38, 123.11, 122.05, 115.71, 70.09.

6.1.4.5. Compound 10: 2-(Phenoxymethyl)benzoic acid. ^{1}H NMR (300 MHz, CDCl₃) δ 11.72 (s, 1H), 8.23 (d, J = 7.8 Hz, 1H), 7.87 (d, J = 7.8 Hz, 1H), 7.65 (s, 1H), 7.45 (s, 1H), 7.38–7.25 (m, 2H), 7.11–6.93 (m, 3H), 5.61 (s, 2H). ^{13}C NMR (75 MHz, CDCl₃) δ 173.87, 159.53, 141.79, 134.68, 132.73, 130.52, 130.48, 128.25, 127.24, 122.00, 115.93, 115.90, 69.02.

6.1.4.6. Compound 13: 1-(Benzyloxy)-2-bromobenzene. ^{1}H NMR (300 MHz, CDCl₃) δ 7.42 (dd, J = 7.8, 1.6 Hz, 1H), 7.33 (d, J = 7.3 Hz, 2H), 7.27–7.10 (m, 3H), 7.02 (dd, J = 7.8, 1.1 Hz, 1H), 6.76–6.61 (m, 2H), 4.90 (s, 2H). ^{13}C NMR (75 MHz, CDCl₃) δ 155.71, 137.26, 134.12, 129.29, 129.20, 128.63, 127.73, 127.71, 122.85, 114.49, 71.29.

6.1.4.7. Compound 14: 2-(Benzyloxy)benzoic acid. ^{1}H NMR (300 MHz, CDCl₃) δ 10.52 (s, 1H), 7.77 (dt, J = 27.4, 13.7 Hz, 2H), 7.36 (d, J = 4.1 Hz, 1H), 7.32 (s, 2H), 7.00 (t, J = 7.5 Hz, 1H), 6.79 (ddd, J = 19.3, 17.3, 8.3 Hz, 3H), 5.15 (s, 2H).

J. D. Majmudar et al. / Bioorg. Med. Chem. 20 (2012) 283–295

293

6.1.4.8. Compound 15: 1-((Benzyloxy)methyl)-2-bromobenzene.
^{1}H NMR (300 MHz, CDCl$_3$) δ 7.62–7.49 (m, 2H), 7.49–7.27 (m, 6H), 7.23–7.08 (m, 1H), 4.69 (s, 4H). ^{13}C NMR (75 MHz, CDCl$_3$) δ 138.97, 138.57, 133.43, 130.06, 129.84, 129.41, 129.37, 128.67, 128.33, 123.68, 73.67, 72.50.

6.1.4.9. Compound 16.
^{1}H NMR (300 MHz, CDCl$_3$) δ 7.72–7.49 (m, 3H), 7.49–7.31 (m, 5H), 7.25–7.11 (m, 1H), 4.73 (s, 4H). ^{13}C NMR (75 MHz, CDCl$_3$) δ 171.87, 137.97, 135.77, 133.43, 130.06, 129.84, 129.41, 129.37, 128.67, 127.45, 123.68, 72.58, 71.65.

6.1.4.10. Compound 17: (S)-2-(2-Phenoxybenzamido)-3-(((2E,6E)-3,7,11-trimethyldodeca-2,6,10-trien-1-yl)thio)propanoic acid.
^{1}H NMR (300 MHz, CDCl$_3$) δ 10.02 (bs, 1H), 8.77 (d, J = 6.7 Hz, 1H), 8.22 (d, J = 7.1 Hz, 1H), 7.35 (t, J = 7.9 Hz, 3H), 7.23–7.04 (m, 4H), 6.83 (d, J = 8.2 Hz, 1H), 5.07 (dd, J = 8.1, 3.9 Hz, 3H), 4.95 (d, J = 5.5 Hz, 1H), 3.18–2.86 (m, 4H), 1.99 (tt, J = 27.6, 13.8 Hz, 8H), 1.64 (d, J = 14.5 Hz, 3H), 1.58 (d, J = 4.3 Hz, 6H), 1.55 (s, 3H). ^{13}C NMR (75 MHz, CDCl$_3$) δ 174.65, 165.04, 155.79, 155.01, 139.55, 134.99, 132.96, 132.15, 131.03, 129.85, 124.49, 124.17, 123.67, 123.26, 122.50, 119.66, 119.41, 117.77, 52.82, 39.52, 39.40, 32.71, 29.74, 26.54, 26.27, 25.55, 17.54, 15.85.

6.1.4.11. Compound 18: (R,E)-3-((3,7-Dimethylocta-2,6-dien-1-yl)thio)-2-(2-phenoxybenzamido)propanoic acid.
^{1}H NMR (300 MHz, CDCl$_3$) δ 10.28 (s, 1H), 8.69 (d, J = 6.6 Hz, 1H), 8.20 (dd, J = 7.8, 1.7 Hz, 1H), 7.36 (dd, J = 10.7, 4.8 Hz, 3H), 7.16 (t, J = 7.4 Hz, 2H), 7.12–7.05 (m, 2H), 6.84 (d, J = 8.2 Hz, 1H), 5.10–4.98 (m, 2H), 4.91 (dd, J = 11.4, 6.0 Hz, 1H), 3.17–2.85 (m, 4H), 2.07–1.88 (m, 4H), 1.64 (s, 3H), 1.54 (d, J = 4.7 Hz, 6H). ^{13}C NMR (75 MHz, CDCl$_3$) δ 174.74, 165.43, 156.12, 155.24, 139.95, 133.33, 132.39, 131.75, 130.15, 124.84, 123.98, 123.55, 122.66, 119.94, 119.64, 118.08, 52.89, 39.63, 32.63, 29.93, 26.51, 25.78, 17.79, 16.09.

6.1.4.12. Compound 19: (R)-2-(2-Phenoxybenzamido)-3-(((2E,6E,10E)-3,7,11,15-tetramethylhexadeca-2,6,10,14-tetraen-1-yl)thio)propanoic acid.
^{1}H NMR (500 MHz, CDCl$_3$) δ 9.73–9.72 (m, 1H), 8.85 (d, J = 6.8 Hz, 1H), 8.03 (dd, J = 7.8, 1.6 Hz, 1H), 7.46–7.32 (m, 3H), 7.18 (td, J = 7.6, 1.0 Hz, 2H), 7.12–7.05 (m, 2H), 6.89–6.82 (m, 1H), 5.16–4.98 (m, 4H), 4.68 (d, J = 4.8 Hz, 1H), 3.16–2.89 (m, 5H), 2.12–1.86 (m, 12H), 1.63 (d, J = 0.9 Hz, 3H), 1.61–1.49 (m, 12H). ^{13}C NMR (126 MHz, CDCl$_3$) δ 177.26, 166.97, 157.50, 157.26, 140.42, 136.37, 136.08, 134.39, 132.73, 132.29, 131.40, 125.96, 125.70, 125.44, 125.36, 124.70, 121.87, 121.20, 119.63, 114.89, 50.10, 41.12, 41.05, 40.93, 34.66, 31.04, 28.07, 27.83, 27.68, 26.19, 18.06, 16.47, 16.43, 16.40.

6.1.4.13. Compound 20: (R)-2-(N-Methyl-2-phenoxybenzamido)-3-(((2E,6E)-3,7,11-trimethyldodeca-2,6,10-trien-1-yl)thio)propanoic acid.
^{1}H NMR (300 MHz, MeOH) δ 7.33–7.11 (m, 4H), 7.10–6.93 (m, 3H), 6.92–6.81 (m, 2H), 6.80–6.56 (m, 1H), 4.94 (d, J = 1.3 Hz, 3H), 4.30–4.13 (m, 1H), 3.12–2.98 (m, 1H), 2.94 (d, J = 7.6 Hz, 1H), 2.87 (d, J = 5.8 Hz, 1H), 2.81 (s, 2H), 2.72 (dd, J = 13.9, 4.2 Hz, 1H), 2.03–1.97 (m, 2H), 1.97–1.75 (m, 8H), 1.51 (s, 4H), 1.44 (s, 6H). ^{13}C NMR (75 MHz, MeOH) δ 171.94, 157.82, 136.14, 132.05, 131.93, 130.91, 130.87, 125.44, 125.38, 125.13, 124.55, 121.60, 121.09, 120.98, 120.36, 119.12, 62.48, 40.84, 40.70, 30.69, 29.84, 27.78, 27.46, 25.97, 17.84, 16.31, 16.24, 16.20.

6.1.4.14. Compound 21: ((R)-2-(2-Phenoxybenzamido)-3-(undecylthio)propanoic acid).
^{1}H NMR (300 MHz, MeOH) δ 7.93 (dd, J = 7.8, 1.7 Hz, 1H), 7.37–7.18 (m, 3H), 7.18–6.93 (m, 4H), 6.88–6.65 (m, 1H), 4.48 (t, J = 5.0 Hz, 1H), 2.94 (ddd, J = 33.3, 13.6, 5.0 Hz, 2H), 2.34 (dd, J = 10.9, 3.9 Hz, 2H), 1.39–1.23 (m, 2H), 1.12 (d, J = 17.7 Hz, 16H), 0.78 (t, J = 6.7 Hz, 3H). ^{13}C NMR (75 MHz, MeOH) δ 178.93, 174.66, 166.37, 157.14, 134.02, 133.69, 132.52, 130.86, 125.56, 124.19, 121.04, 119.56, 37.67, 35.60, 33.33, 33.05, 30.97, 30.81, 30.74, 30.71, 30.49, 23.49, 14.39, 5.36.

6.2. Materials and methods

6.2.1. Materials
N-2-Phenoxybenzoyl-S-3-(3-methyl-but-2-enyl)-5-(4-biphenyl)-pent-2-enyl-L-cysteine (POP-3MB, compound **1b**) was synthesized in our laboratory[25] via established solution-phase methods and characterized to confirm identity and purity. Stock solutions were prepared at 50 mM in DMSO and stored at −80 °C. EGFP-C3 vectors containing GFP K-Ras was a generous gift from Mark Philips (New York University, School of Medicine). pGEX vector containing GST-RBD was a kind gift from Lawrence Quilliam (Indiana University School of Medicine). The following antibodies were used: Pan Ras (Oncogene, OP40), Phospho-p44/42 MAPK (Erk1/2) (Thr202/Tyr204) (197G2) Rabbit mAb (Cell Signaling Technology, 4377L), GAPDH (Ambion, 4300), CD-3ε (UCHT1) (BD Pharmingen, 555329), ImmunoPure Goat Anti-Rabbit IgG, Peroxidase Conjugated (GARP, Pierce Biotechnology, 31462), ImmunoPure Goat Anti-Mouse IgG, Peroxidase Conjugated (GAMP, Pierce Biotechnology, 31432). Formaldehyde 37% solution was purchased from Mallinckrodt.

6.2.2. Cell culture
Jurkat T cells (E 6.1) were obtained and maintained as described previously.[41] For all experiments, cells were treated using a vehicle (DMSO) or drug (diluted from a 50 mM DMSO stock solution) at indicated concentrations for 24 h.

6.2.3. Fluorescence microscopy
Jurkat T cells (1.5 × 107 cells/500 µl RPMI), transiently transfected with 20 µg of either GFP-K-Ras construct (a kind gift from M. Phillips) using the Cell Porator (Life Technologies, 800 µF, 250 V, low ohms), were treated with delivery group (DMSO), simvastatin alone (20 µM), or various concentrations of POP-3 MB (0.1, 1 or 10 µM) for 24 h in an incubator at 37 °C. The cells were harvested, washed with PBS three times, and plated on polylysine coverslips for 10 min. The coverslips were washed with PBS for 10 min (3 times) and the cells were fixed with 3% formaldehyde for 10 min. The coverslips were washed again for 10 min with PBS (3 times). After mounting the coverslips onto the slides using FluorSave™ Reagent (Calbiochem), the slides were dried for 45 min at room temperature. Images of cells were viewed using an Olympus BH-2 microscope and captured with a QImaging Microimager II. The captured images were viewed using Northern Eclipse software. Cells were classified as either full (fully mislocalized GFP-K-Ras construct with diffuse cellular staining), partial (partial proper localization), and normal (normal, primarily plasma membrane localization of GFP-K-Ras) by visual inspection.[40,41] The subcellular localization of GFP K-Ras was quantified using fluorescence microscopy (performed on an Olympus BH-2RFCA) as previously described.[23,50]

6.2.4. Isolation of membrane fraction from yeast cells
Membrane fractions from yeast cells were isolated as previously described.[5] Crude membrane protein concentration was determined using Coomassie Plus Protein Assay Reagent (Pierce) according to the manufacturer's instructions, and compared with a bovine serum albumin standard curve.

6.2.5. Substrate and inhibition assays by in vitro vapor diffusion methyltransferase assay
Methyltransferase assays were performed as previously described[5,38,39] with minor modifications. The assay mixture con-

tained a total volume of 60 μL and a final Tris–HCl buffer concentration of 100 mM, pH 7.5. All reactions contained 20 μM S-adenosyl-[^{14}C-methyl]methionine (^{14}C-SAM) and 5 μg of membrane protein from His-hIcmt-overexpressing strain CH 2766.[5] Initial substrate screening was performed at a single concentration of 25 μM in duplicate, three times. For inhibition screening, protein and compound (10 μM) were pre-incubated on ice in buffer, followed by the addition of 25 μM AFC substrate and ^{14}C-SAM. Reactions were incubated at 30 °C for 30 min and stopped by the addition of 50 μL of 1 M NaOH/1% SDS. 100 μL of this mixture was spotted on folded filter paper (6 cm × 2 cm) and lodged in the neck of a scintillation vial containing 10 mL of scintillation fluid, and capped to allow for diffusion of the released [^{14}C]methanol into the scintillant. The filters were pulled out after 2.5 h, the vials tightly recapped and shaken, and then counted in a liquid scintillation analyzer.

6.2.6. Immunoblotting

Jurkat T cells (3–5 × 10^5 cells mL^{-1}) were treated with vehicle (DMSO), simvastatin, or POP-3 MB (**1a**). Cells were lysed in 1% Triton X-100 lysis buffer (25 mM Hepes, pH 7.2, 150 mM NaCl, 1% NP40, 5 mM EDTA, 10 μg mL^{-1} of leupeptin and aprotinin, and 1 mM sodium vanadate), resolved on SDS–PAGE gels, resolved by SDS–PAGE on 12% gels and transferred to polyvinylidene difluoride membranes (Immun-Blot PVDF; Bio-Rad). Membranes were blocked with 5% goat serum and incubated with primary antibody (anti-Pan Ras (Oncogene OP40) for N/K Ras; or anti-GAPDH (Ambion 4300) for GAPDH at room temperature for 1 h, followed by incubation with horseradish peroxidase-conjugated goat anti-mouse or goat anti-rabbit IgG. Membranes were developed using enhanced chemiluminescence reagents (ECL; Amersham Pharmacia Biotech) and autoradiography film. Quantitative western blotting was performed using ImageJ system.

6.2.7. Signaling assay

Jurkat T cells (1 × 10^7 cells/1 ml) were washed in PBS, incubated with anti-CD-3ε (20 μg/ml) for 15 min on ice, and stimulated at 37 °C for 10 min. Cells were washed and lysed in lysis buffer containing 1% Triton X-100, 20 mM Tris/HCl, pH 7.6, 150 mM NaCl, 20 μg/ml each of leupeptin and aprotinin, 1 mM pyrophosphate, 1 mM glycerol phosphate, and 1 mM sodium orthovanadate. Samples were separated on 6–15% gradient SDS–polyacrylamide gels and analyzed by immunoblotting with anti-phosphoERK antibodies (at 4 °C overnight with anti-p-Erk (Cell Signaling Technology 4377L)). Membranes were developed using enhanced chemiluminescence reagents (ECL; Amersham Pharmacia Biotech) and autoradiography film. Quantitative western blotting was performed using ImageJ system.

6.2.8. GST-RBD pull down assay

GST-RBD fusion protein was expressed in bacteria as previously described.[51] After stimulation with anti CD3 antibody, Jurkat T cells (2 × 10^7) were lysed in 1% NP40 lysis buffer (1% Nonidet P-40, 25 mM HEPES, 150 mM NaCl, 0.25% sodium deoxycholate, 10% glycerol, 10 mM MgCl$_2$, 1 mM EDTA, 1 mM sodium vanadate, 10 mM NaF, 20 g/ml aprotinin and leupeptin, pH 7.4) and centrifuged at 464 × g for 3 min at 4 °C. The lysate was incubated with GST-RBD fusion protein conjugated glutathione-sepharose 4B beads for 30 min at 4 °C. The resin was washed three times with magnesium lysis buffer (25 mM HEPES, pH 7.5, 150 mM NaCl, 1% NP-40, 0.25% sodium deoxycholate 10% glycerol, 10 mM MgCl$_2$), solubilized in 2× PSB (protein sample buffer, protein sample buffer = 100 mM Tris–Hcl, pH 6.8, 20% glycerol, 4%SDS, 0.2% bromophenol blue, 200 mM dithiothreitol) and the presence of activated Ras was detected by immunoblot analysis and quantified using the ImageJ system as mentioned above.

Supplementary data

Supplementary data associated with this article can be found, in the online version, at doi:10.1016/j.bmc.2011.10.087.

References and notes

1. Gelb, M. H.; Brunsveld, L.; Hrycyna, C. A.; Michaelis, S.; Tamanoi, F.; Van Voorhis, W. C.; Waldmann, H. *Nat. Chem. Biol.* **2006**, *2*, 518.
2. Bergo, M. O.; Gavino, B. J.; Hong, C.; Beigneux, A. P.; McMahon, M.; Casey, P. J.; Young, S. G. *J. Clin. Invest.* **2004**, *113*, 539.
3. Winter-Vann, A. M.; Casey, P. J. *Nat. Rev. Cancer* **2005**, *5*, 405.
4. Young, S. G.; Clarke, S. G.; Bergo, M. O.; Phillips, M.; Fong, L. G. *The Enzymes* **2006**, *24*, 273.
5. Anderson, J. L.; Frase, H.; Michaelis, S.; Hrycyna, C. A. *J. Biol. Chem.* **2005**, *280*, 7336.
6. Dai, Q.; Choy, E.; Chiu, V.; Romano, J.; Slivka, S. R.; Steitz, S. A.; Michaelis, S.; Philips, M. R. *J. Biol. Chem.* **1998**, *273*, 15030.
7. Clarke, S. *Ann. Rev. Biochem.* **1992**, *61*, 355.
8. Zhang, F. L.; Casey, P. J. *Ann. Rev. Biochem.* **1996**, *65*, 241.
9. Basso, A. D.; Kirschmeier, P.; Bishop, W. R. *J. Lipid Res.* **2006**, *47*, 15.
10. Otto, J. C.; Kim, E.; Young, S. G.; Casey, P. J. *J. Biol. Chem.* **1999**, *274*, 8379.
11. Bergo, M. O.; Leung, G. K.; Ambroziak, P.; Otto, J. C.; Casey, P. J.; Gomes, A. Q.; Seabra, M. C.; Young, S. G. *J. Biol. Chem.* **2001**, *276*, 5841.
12. Bergo, M. O.; Leung, G. K.; Ambroziak, P.; Otto, J. C.; Casey, P. J.; Young, S. G. *J. Biol. Chem.* **2000**, *275*, 17605.
13. Cohen, S. J.; Ho, L.; Ranganathan, S.; Abbruzzese, J. L.; Alpaugh, R. K.; Beard, M.; Lewis, N. L.; McLaughlin, S.; Rogatko, A.; Perez-Ruixo, J. J.; Thistle, A. M.; Verhaeghe, T.; Wang, H.; Weiner, L. M.; Wright, J. J.; Hudes, G. R.; Meropol, N. J. *J. Clin. Oncol.* **2003**, *21*, 1301.
14. Macdonald, J. S.; McCoy, S.; Whitehead, R. P.; Iqbal, S.; Wade, J. L., 3rd; Giguere, J. K.; Abbruzzese, J. L. *Invest. New Drugs* **2005**, *23*, 485.
15. Van Cutsem, E.; van de Velde, H.; Karasek, P.; Oettle, H.; Vervenne, W. L.; Szawlowski, A.; Schoffski, P.; Post, S.; Verslype, C.; Neumann, H.; Safran, H.; Humblet, Y.; Perez Ruixo, J.; Ma, Y.; Von Hoff, D. *J. Clin. Oncol.* **2004**, *22*, 1430.
16. Whitehead, R. P.; McCoy, S.; Macdonald, J. S.; Rivkin, S. E.; Neubauer, M. A.; Dakhil, S. R.; Lenz, H. J.; Tanaka, M. S.; Abbruzzese, J. L. *Invest. New Drugs* **2006**, *24*, 335.
17. Whyte, D. B.; Kirschmeier, P.; Hockenberry, T. N.; Nunez-Oliva, I.; James, L.; Catino, J. J.; Bishop, W. R.; Pai, J. K. *J. Biol. Chem.* **1997**, *272*, 14459.
18. Adjei, A. A. *J. Natl. Cancer Inst.* **2001**, *93*, 1062.
19. Rowell, C. A.; Kowalczyk, J. J.; Lewis, M. D.; Garcia, A. M. *J. Biol. Chem.* **1997**, *272*, 14093.
20. Michaelson, D.; Ali, W.; Chiu, V. K.; Bergo, M.; Silletti, J.; Wright, L.; Young, S. G.; Philips, M. *Mol. Biol. Cell* **2005**, *16*, 1606.
21. Volker, C.; Lane, P.; Kwee, C.; Johnson, M.; Stock, J. *FEBS Lett.* **1991**, *295*, 189.
22. Roberts, P. J.; Mitin, N.; Keller, P. J.; Chenette, E. J.; Madigan, J. P.; Currin, R. O.; Cox, A. D.; Wilson, O.; Kirschmeier, P.; Der, C. J. *J. Biol. Chem.* **2008**, *283*, 25150–25163.
23. Wang, M.; Tan, W.; Zhou, J.; Leow, J.; Go, M.; Lee, H. S.; Casey, P. J. *J. Biol. Chem.* **2008**, *283*, 18678–18684.
24. Wahlstrom, A. M.; Cutts, B. A.; Liu, M.; Lindskog, A.; Karlsson, C.; Sjogren, A. K.; Andersson, K. M.; Young, S. G.; Bergo, M. O. *Blood* **2008**, *112*, 1357–1365.
25. Donelson, J. L.; Hodges-Loaiza, H. B.; Henriksen, B. S.; Hrycyna, C. A.; Gibbs, R. A. *J. Org. Chem.* **2009**, *74*, 2975.
26. Tan, E. W.; Perez-Sala, D.; Canada, F. J.; Rando, R. R. *J. Biol. Chem.* **1991**, *266*, 10719.
27. Volker, C.; Lane, P.; Kwee, C.; Johnson, M.; Stock, J. *FEBS Lett.* **1991**, *295*, 189.
28. Volker, C.; Miller, R. A.; McCleary, W. R.; Rao, A.; Poenie, M.; Backer, J. M.; Stock, J. B. *J. Biol. Chem.* **1991**, *266*, 21515.
29. Perez-Sala, D.; Gilbert, B. A.; Tan, E. W.; Rando, R. R. *Biochem. J.* **1992**, *284*(Pt 3), 835.
30. Henriksen, B. S.; Anderson, J. L.; Hrycyna, C. A.; Gibbs, R. A. *Bioorg. Med. Chem. Lett.* **2005**, *15*, 5080.
31. Tan, E. W.; Rando, R. R. *Biochemistry* **1992**, *31*, 5572.
32. Stephenson, R. C.; Clarke, S. *J. Biol. Chem.* **1990**, *265*, 16248.
33. Anderson, J. L.; Henriksen, B. S.; Gibbs, R. A.; Hrycyna, C. A. *J. Biol. Chem.* **2005**, *280*, 29454.
34. Donelson, J. L.; Hodges, H. B.; MacDougall, D. D.; Henriksen, B. S.; Hrycyna, C. A.; Gibbs, R. A. *Bioorg. Med. Chem. Lett.* **2006**, *16*, 4420.

35. Bonnet, B.; Soullez, D.; Girault, S.; Maes, L.; Landry, V.; Davioud-Charvet, E.; Sergheraert, C. *Bioorg. Med. Chem.* **2000**, *8*, 95.
36. Majmudar, J. D.; Hahne, K.; Hrycyna, C. A.; Gibbs, R. A. *Bioorg. Med. Chem. Lett.* **2011**, *21*, 2616.
37. Ruggles, E. L.; Flemer, S.; Hondal, R. J. *Biopolymers* **2008**, *90*, 61.
38. Hrycyna, C. A.; Yang, M. C.; Clarke, S. *Biochemistry* **1994**, *33*, 9806.
39. Hrycyna, C. A.; Clarke, S. *Mol. Cell Biol.* **1990**, *10*, 5071.
40. Choy, E.; Philips, M. *Methods in Enzymology, Part F* **2001**, *332*, 50.
41. Krzysiak, A. J.; Rawat, D. S.; Scott, S. A.; Pais, J. E.; Handley, M.; Harrison, M. L.; Fierke, C. A.; Gibbs, R. A. *ACS Chem. Biol.* **2007**, *2*, 385.
42. Perez de Castro, I.; Bivona, T. G.; Philips, M. R.; Pellicer, A. *Mol. Cell Biol.* **2004**, *24*, 3485.
43. Castro, A. F.; Rebhun, J. F.; Quilliam, L. A. *Methods* **2005**, *37*, 190.
44. Winter-Vann, A. M.; Baron, R. A.; Wong, W. H.; dela Cruz, J.; York, J. D.; Gooden, D. M.; Bergo, M. O.; Young, S. G.; Toone, E. J.; Casey, P. J. *Proc. Natl. Acad. Sci. U.S.A.* **2005**, *102*, 4336.
45. Tsimberidou, A. M.; Rudek, M. A.; Hong, D.; Ng, C. S.; Blair, J.; Goldsweig, H.; Kurzrock, R. *Cancer Chemother. Pharmacol.* **2010**, *65*, 235.
46. Haklai, R.; Elad-Sfadia, G.; Egozi, Y.; Kloog, Y. *Cancer Chemother. Pharmacol.* **2008**, *61*, 89.
47. Jansen, B.; Schlagbauer-Wadl, H.; Kahr, H.; Heere-Ress, E.; Mayer, B. X.; Eichler, H. G.; Pehamberger, H.; Gana-Weisz, M.; Ben-David, E.; Kloog, Y.; Wolff, K. *Proc. Natl. Acad. Sci. U.S.A.* **1999**, *96*, 14019.
48. Judd, W. R.; Slattum, P. M.; Hoang, K. C.; Bhoite, L.; Valppu, L.; Alberts, G.; Brown, B.; Roth, B.; Ostanin, K.; Huang, L.; Wettstein, D.; Richards, B.; Willardsen, J. A. *J. Med. Chem.* **2011**, *54*, 5031.
49. Brown, M. J.; Milano, P. D.; Lever, D. C.; Epstein, W. W.; Poulter, C. D. *J. Am. Chem. Soc.* **1991**, *113*, 3176.
50. McCabe, J. B.; Berthiaume, L. G. *Mol. Biol. Cell* **1999**, *10*, 3771.
51. Castro, A. F.; Rebhun, J. F.; Quilliam, L. A. *Methods (San Diego, Calif)* **2005**, *37*, 190.
52. Robert, A. *Evaluation of Enzyme Inhibitors in Drug Discovery: A Guide for Medicinal Chemists and Pharmacologists*; Wiley Press: Copeland, 2005. 131.
53. Cer, R. Z.; Mudunuri, U.; Stephens, R.; Lebeda, F. J. *Nucleic Acids Res.* **2009**, *37*, W441–W445.